LANGMUIR

Article

pubs.acs.org/Langmuir

Enhanced Response Time of Electrowetting Lenses with Shaped Input Voltage Functions

Omkar D. Supekar,*[,†,‡] Mo Zohrabi,[†,§] Juliet T. Gopinath,[§] and Victor M. Bright[‡]

[‡]Department of Mechanical Engineering and [§]Department of Electrical, Computer, and Energy Engineering, University of Colorado, Boulder, Colorado 80309, United States

ABSTRACT: Adaptive optical lenses based on the electrowetting principle are being rapidly implemented in many applications, such as microscopy, remote sensing, displays, and optical communication. To characterize the response of these electrowetting lenses, the dependence upon direct current (DC) driving voltage functions was investigated in a low-viscosity liquid system. Cylindrical lenses with inner diameters of 2.45 and 3.95 mm were used to characterize the dynamic behavior of the liquids under DC voltage electrowetting actuation. With the increase of the rise time of the input exponential driving voltage, the originally underdamped system response can be damped, enabling a smooth response from the lens. We experimentally determined the optimal rise times for the fastest response from the lenses. We have also performed numerical simulations of the lens actuation with input exponential driving voltage to understand the variation in the dynamics of the liquid−liquid interface with various input rise times. We further enhanced the response time of the devices by shaping the input voltage function with multiple exponential rise times. For the 3.95 mm inner diameter lens, we achieved a response time improvement of 29% when compared to the fastest response obtained using single-exponential driving voltage. The technique shows great promise for applications that require fast response times.

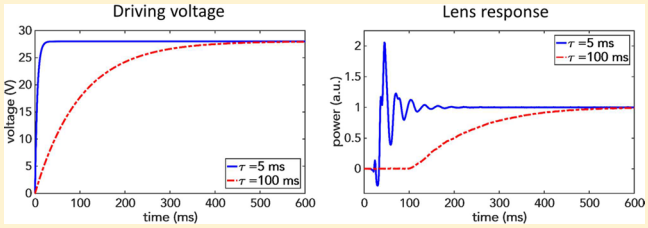

INTRODUCTION

The electrowetting on dielectric (EWOD)[1] principle enables the control of the shape of a liquid droplet or liquid−liquid interface on a dielectric surface through an applied voltage. The result is an ultrasmooth, tunable liquid interface that is an ideal platform for tunable lenses and prisms.[1−3] Devices based on the EWOD principle are appealing as a result of their low power consumption, large range of tunability, and no mechanical moving parts. Recently, an optical switch with a high rejection ratio has been demonstrated with this technology.[4] Other applications include flexible lenses[5] and lens arrays,[6] multifunctional lenses for miniature cameras,[7,8] optical displays,[9,10] lab-on-a-chip systems,[11] and micro total analysis systems for biological applications, such as polymerase chain reactions,[12,13] deoxyribonucleic acid (DNA) enrichment, and cell assays.

Understanding the temporal dynamics of EWOD devices, especially the response time, is important for many applications. Recently, microscopes incorporating EWOD lenses have been demonstrated, enabling non-mechanical depth scanning.[14,15] EWOD prisms have also been used for non-mechanical beam steering[3] and show promise for light detection and ranging (LIDAR) and remote sensing applications. The technology also shows promise for consumer market applications, such as optical switches[4,16,17] for communications and display[9,10] technologies. However, achieving fast response times from these devices is one of the main challenges. For instance, a typical confocal microscope uses a pair of galvanometer mirrors for two-dimensional (2D) lateral scans at kilohertz frequencies. Using a liquid lens in such a microscope would allow for a large depth scan; however, the response time of such an element needs to be comparable to the lateral scanning speed.[15,18] Another example of a different technology is an optical switch based on a digital micromirror device (DMD). These optical switches have been developed and used for wavelength division multiplexing with a switching time of 15 μs.[19] To replace conventional adaptive optical elements, EWOD devices need a path to comparable response time.

To optimize the response of EWOD devices, it is imperative to study the dynamics of the liquid motion upon actuation. This dynamic behavior of EWOD actuation has been studied for droplet spreading,[20−22] capillary rise,[23,24] and lenses,[25−27] with particular emphasis on numerical modeling along with understanding the material properties and dimensional dependence of the actuation dynamics. For example, Hong et al.[21] investigated the effect of the droplet size and viscosity on the droplet spreading dynamics under direct current (DC) voltage actuation. This study showed that the droplet response time (aqueous 1 mM NaCl solution), with droplet sizes below the capillary length of the solutions under EWOD actuation, has a $r^{1.5}$ dependence, where r is the effective base radius of the droplet. Additionally, by increasing the viscosity of the droplet, the response time can be tuned from underdamped to overdamped. Alternatively, for EWOD systems with viscous fluids, an overdrive voltage technique has been demonstrated to enhance the response in droplet spreading,[22] capillary rise,[23] and lenses.[25] Kuiper and Hedriks,[27] in their study, have

Received: February 23, 2017
Revised: April 18, 2017
Published: April 21, 2017

DOI: 10.1021/acs.langmuir.7b00631
Langmuir 2017, 33, 4863−4869

reported systems with both underdamped and overdamped characteristics and, on the basis of a damped spring-mass system model, derived dimensionless parameters to calculate the necessary liquid viscosity for a given lens dimension for critically damped lens operation. Recently, studies were published on the response and the aperture size of EWOD lenses.[25,26]

Here, we focus on a systematic study of the response time of a cylindrical geometry EWOD lens rather than a droplet and the device dependence upon DC input voltage shape. This systematic approach enables us to determine the optimal driving voltage shape for the fastest response from an EWOD lens, without changing the physical properties of the lens (such as viscosity and density of the liquids). For this purpose, an exponential voltage function with variable input rise time is used to study the dynamic behavior of our devices. The response time is further enhanced using a shaped voltage consisting of a combination of two exponential input voltage functions. In addition, we have also performed 2D axisymmetric finite element simulations to study the interface dynamics upon actuation and compared to our experimental results.

The static response of an EWOD lens before the onset of contact angle saturation can be described by the Lippmann–Young equation,[1,28] $\cos\theta = \cos\theta_0 + (\epsilon\epsilon_0/2\gamma d)V^2$, where θ is the contact angle upon applying a voltage V, θ_0 is the initial contact angle without any applied voltage, ϵ and d are the effective dielectric constant and thickness of the dielectric layers, and γ is the surface tension of the liquid–liquid interface. The schematic of an oil–water EWOD lens is shown in Figure 1.

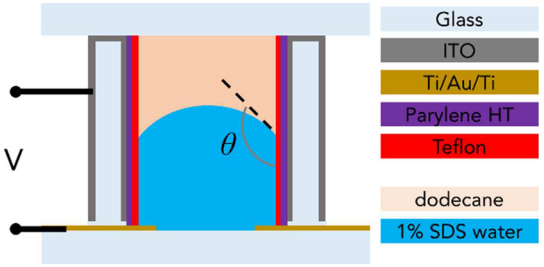

Figure 1. Schematic of an oil–water EWOD liquid lens with an electrode on the base and a hydrophobic coating, a dielectric layer, and an electrode along the sidewalls. A cylindrical glass tube is coated with an ITO electrode, a Parylene HT dielectric, and a Teflon hydrophobic coating. The glass tube is epoxy-bonded to an optical window with annular electrode pattern, and a cover glass slip seals the device after filling the device with the liquids. Voltage, V, denotes the applied voltage on the sidewall electrodes. The lens is filled with 1 wt % SDS water solution (n = 1.33) and dodecane (n = 1.421).

The dielectric layer is coated with a hydrophobic surface first to enhance the initial contact angle to provide a high tunable range and second to reduce contact angle hysteresis. The motion of the contact line on this hydrophobic surface has a strong influence over the response characteristics of EWOD lenses and can be modeled as a fluid slip boundary condition with an applied friction force proportional to the fluid velocity.[20] In this work, the fluid slip is modeled using a Navier-slip boundary condition. The response time of the EWOD lenses also depends upon the physical properties of the fluids, such as density and viscosity, and surface tension between the liquids. In our study, the physical properties of the liquids and the dielectric properties of the insulating layer are kept fixed. The polar liquid used is a 1 wt % sodium dodecyl sulfate (SDS) aqueous solution, and the nonpolar liquid used is dodecane. Water has a viscosity of 0.89 mPa s, and dodecane has a viscosity of 1.36 mPa s. The interfacial surface tension between the liquids is 5.7 mN/m,[29] resulting in an underdamped system.

EXPERIMENTAL DETAILS

Our EWOD lens design is simple, compatible with standard microfabrication techniques, and based on the process flow described by Kuiper and Hendriks.[27] Cylindrical glass tubes (inner diameters of 2.45 and 3.95 mm, corresponding to heights of 3 and 5 mm, respectively) are used to construct our electrowetting lenses. A schematic of the EWOD liquid lens device studied is shown in Figure 1. The cylindrical glass tube is coated with indium tin oxide (ITO) as the electrode layer, using a DC sputter system. The chamber was first pumped down to a base pressure of 1 μTorr, followed by the introduction of argon gas into the chamber. The deposition was performed at a pressure of 8 mTorr and a power of 120 W. A 300 nm layer of ITO was deposited at an average rate of 3.33 Å/s, as measured by a quartz crystal microbalance. These deposition parameters were experimentally determined to ensure continuous electrode deposition on the vertical sidewalls of the glass tube. Before the dielectric layers are deposited, the exterior of the glass tubes is masked with Kapton tape. Next, the inner sidewalls of the tubes are coated with a 1 μm Parylene HT layer using vapor-phase deposition (Specialty Coating Systems). The devices are then dip-coated in a 1 wt % solution of Teflon (DuPont AF1600) in Fluorinert FC-40 and cured at 170 °C for 20 min. The Kapton tape used for masking is removed, and the glass tube is epoxy-bonded to an optical window that is patterned with an annular titanium/gold/titanium (Ti/Au/Ti) electrode, which serves as the ground electrode for the lens. The annular-patterned optical windows are fabricated using the lift-off technique. A negative of the pattern is first generated on the optical window with negative photoresist NR7-1500 PY (Futurrex, Inc.), followed by evaporating Ti/Au/Ti (10/500/10 nm) on the optical window. The optical window is then dipped in acetone to dissolve the underlying photoresist, leading to an annular electrode pattern on the optical window. Finally, the lenses are filled with the polar liquid (1 wt % SDS solution), followed by the nonpolar liquid (dodecane).

A laser beam from a 785 nm continuous wave (cw) laser diode is spatially filtered and collimated to 0.5 mm diameter. The beam is passed through the axis of the electrowetting lens, as shown in Figure 2a. A 400 μm aperture and a photodiode (Thorlabs DET10A) are placed after the lens, and the resulting electrical signal is recorded using a data acquisition card (DAQ). This technique allows for the characterization of EWOD lenses without a high-speed camera, generating a time-dependent signal that can be related to the dynamics of the liquid–liquid interface itself. At the liquid–liquid interface of the 1 wt % SDS water solution (n = 1.33) and dodecane (n = 1.421), a concave spherical lens is generated. This results in a divergent output beam from the lens. The focal length of the lens can be tuned upon actuation, and for this purpose, a signal from an arbitrary waveform generator (Agilent 33250A) is amplified (Thorlabs MDT694) to generate the input-shaped drive voltages and applied to the electrodes of the lens. An example of exponential input voltages, $V = V_0(1 - e^{-t/\tau})$, is shown in Figure 2b for input rise times of 5 and 20 ms. A typical DC power supply can generate outputs with rise times from a few to hundreds of milliseconds.

The steady-state contact angles with applied voltage were experimentally determined to be 155° at 0 V and 90° at 28 V DC (see Figure 2c). The lenses were actuated from an initial contact angle of 155° to 90°. This contact angle variation covers the full range of operation as a diverging lens, and ensures repeatable and consistent experiments. The change in the curvature of the liquid–liquid interface with the input voltage function changes the intensity of the beam through the aperture as a function of time. This intensity variation with time is captured by the photodiode. For example, the photodiode signal for a 3.95 mm inner diameter device as a function of time for various input exponential rise times is shown in Figure 3. It is evident from the figure that, for an input rise time of 5–20 ms, the photodiode

DOI: 10.1021/acs.langmuir.7b00631
Langmuir 2017, 33, 4863–4869

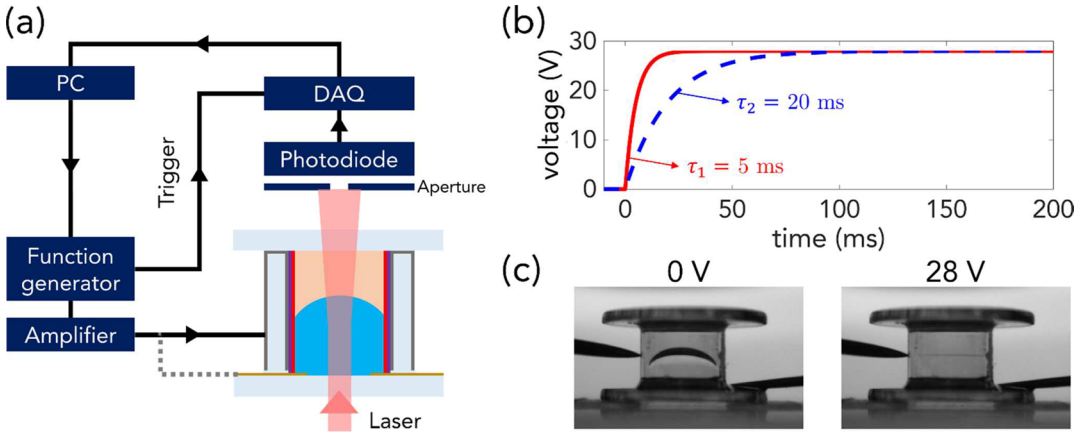

Figure 2. (a) Schematic diagram of the experimental setup. Arbitrary-shaped voltage inputs are generated using an Agilent 33250A function generator and amplified to drive the EWOD lens. A laser beam is passed through the axis of the lens and is collected on a photodiode, after an aperture. DAQ = data acquisition card. (b) Exponential input voltages, $V = V_0(1 - e^{-t/\tau})$, generated using an arbitrary waveform generator with rise times of 5 and 20 ms. (c) Electrowetting lens device with unshaped applied DC voltages of 0 and 28 V.

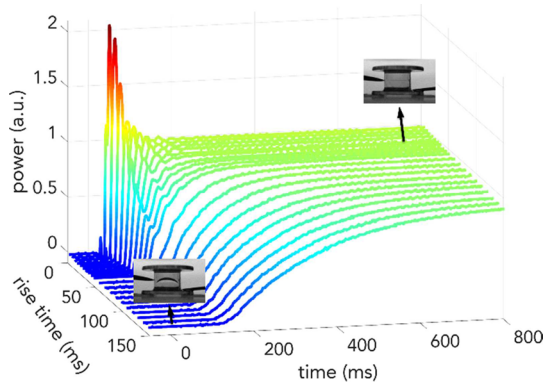

Figure 3. Normalized photodiode signal as a function of time for various input exponential rise times. The input rise times of the exponential voltages are swept from 5 to 150 ms with voltage amplitude changes from 0 to 28 V. The color represents the signal strength on the photodiode.

signal has under damped oscillation characteristics; however, these oscillations are suppressed and transition to overdamped characteristics for larger input exponential rise times of 50–150 ms.

SIMULATION DETAILS

To study the dynamics of the liquid–liquid interface in the EWOD lens, COMSOL Multiphysics 5.2a is used. We have modeled our devices using the 2D axisymmetric, two-phase laminar flow module. A moving mesh boundary is employed to simulate the liquid–liquid interface motion. The response characteristics of EWOD devices are simulated for various applied input rise times. The experimentally measured initial contact angle was used as an initial geometric condition in the simulation. Figure 4 shows a detailed schematic of the boundary conditions and the simulation setup. The experimentally determined contact angle variation as a function of voltage was provided as the boundary condition at the contact line in the form of Lippmann–Young's equation.[1,28] One outcome of our simulation is the time-dependent evolution of the liquid–liquid interface.

The sliding of the contact line on the sidewall of the lens is modeled using a Navier-slip condition. This boundary condition applies a friction force opposing the sliding of the liquid–liquid interface on the sidewall. The associated Navier-slip

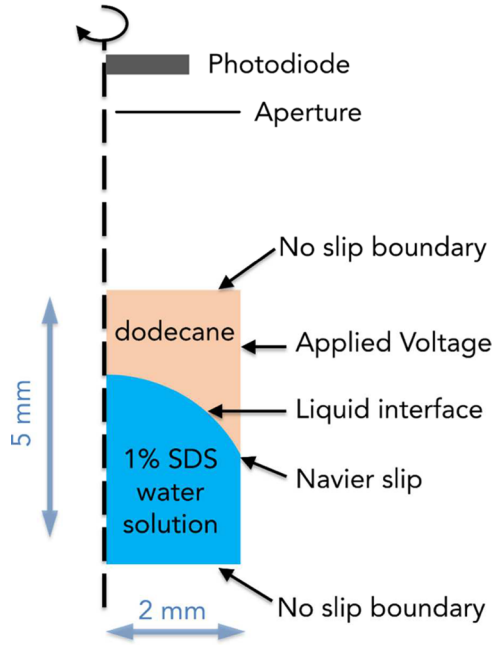

Figure 4. Schematic of the COMSOL 5.2a model geometry. A 2D axisymmetric condition is used and a Navier slip boundary condition is applied to the wall at the contact line. Starting with an initial contact angle of 155° (experimentally measured), the response of the system for an applied exponential voltage, $V = V_0(1 - e^{-t/\tau})$, is simulated using various input rise times. SDS = sodium dodecyl sulfate.

length parameter governs the magnitude of this friction force and has a strong influence on the dynamics of the contact line motion and, successively, the dynamics of the liquid–liquid interface upon a time-dependent voltage actuation. To determine this slip length parameter, the simulation was compared to the experimental results using the COMSOL Ray optics module.

In our simulation, a 785 nm laser beam with Gaussian profile was passed through the axis of the device. We use the previously simulated dynamic response of the liquid–liquid interface surface to predict the time-dependent photodiode response. By comparing the simulation to experimental results, the slip length parameter was determined to be 1000 nm. The slip length parameter is in agreement with theoretical prediction,

DOI: 10.1021/acs.langmuir.7b00631
Langmuir 2017, 33, 4863–4869

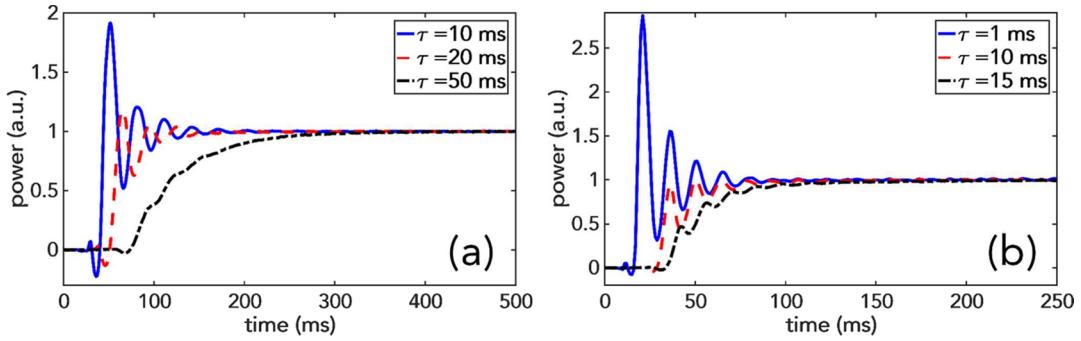

Figure 5. Experimental response characteristics of (a) 3.95 mm and (b) 2.45 mm lenses for different input exponential rise times. The oscillations suppress with increasing the input exponential rise time.

because the slip length increases as the hydrophobicity of the surface increases and slip lengths of the order of micrometers can be obtained for superhydrophobic surfaces.[30]

RESULTS AND DISCUSSION

Effect of the Exponential Rise Time. The EWOD lens response was first characterized using an exponential input voltage, $V = V_0(1 - e^{-t/\tau})$, with varying rise times. The lenses were actuated from an initial contact angle of 155° at 0 V to 90° at 28 V. Upon actuation, the resulting variation of the contact angle with applied voltage leads to significant contact line motion, which generates a standing wave in the lens that, over time, propagates to the axis of the lens. The settling time for the generated standing wave is strongly dependent upon the interfacial surface tension, viscosity of the liquids, and shape of the driving voltage. For a given viscosity and surface tension, the standing wave generated at the liquid–liquid interface strongly depends upon the driving input voltage. As a result, the lens response can be characterized as underdamped or overdamped on the basis of the driving input voltage. The liquids used in the lenses have a low viscosity (<2 mPa s), leading to a significant settling time (approximately 150 ms) for the generated standing wave from a short rise time input exponential voltage. The standing wave oscillations can be suppressed by reducing the contact line velocity through applied input voltage function. The experimental response of the 3.95 and 2.45 mm inner diameter lenses is characterized in Figure 5. Figure 5a shows the 3.95 mm diameter lens with exponential input rise times of 10, 20, and 50 ms. The input rise times of 10 and 20 ms result in multiple oscillations at the liquid–liquid interface, showing the characteristics of an underdamped system. For a longer input rise time of 50 ms, the liquid–liquid interface follows the input voltage shape. The oscillations in the lens response are suppressed; however, the response time of the lens is increased when compared to the response from 10 and 20 ms input rise time. Figure 5b depicts a similar behavior for a 2.45 mm diameter lens using input rise times of 1, 10, and 15 ms.

Figure 6 shows the variation of the response time in the 3.95 mm inner diameter lens as a function of the input voltage rise time. The response time (settling time) of the lens was calculated as the time taken for the photodiode signal to settle within 2.5% (above the noise floor of the measurement) of its steady-state signal. The response time curve for the 3.95 mm lens has a local minimum, showing an optimal input voltage rise time for fast response from the lens. The fastest response for the 3.95 mm lens was 138 ms for an input rise time of 15 ms. For the 2.45 mm lens, no such local minima was observed and a

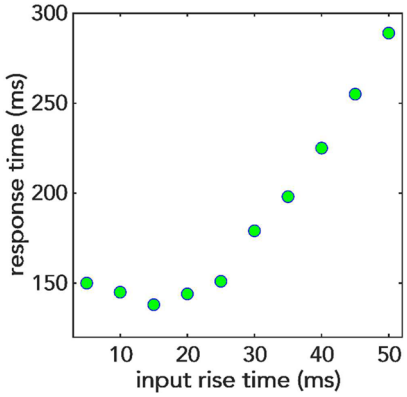

Figure 6. Response time variation of the 3.95 mm lens as a function of input exponential rise time. The response time is determined from the photodiode signal settling within 2.5% of its steady-state signal.

response time of 88 ms for an input rise time of 1 ms was the best result. Even though rise time did not have any effect on enhancing the response time of the 2.45 mm lens, the oscillations at the interface are suppressed with an increasing rise time, enabling a smoother response from the lens. The degree of contact line motion depends upon the diameter of the cylindrical glass tube. For a smaller diameter glass tube, the contact line motion will be smaller, resulting in a lens with a faster response time.

As shown in Figure 5, there is a small delay between the input voltage (starting at the origin) and the lens response. Additionally, this delay increases for larger rise time input voltages. This delay in the response time of the lens can be explained as a combination of (1) the propagation time for the standing wave to reach the center of the lens and (2) the inherent *RC* (resistance and capacitance) time constant of the device. The former is governed by the fluid dynamics, while the latter is a result of the device electrode, dielectric material, and liquid properties.

The contact line motion is determined by the contact angle variation, which has a squared dependence upon the applied voltage (Lippmann–Young equation[1,28]). This means that noticeable contact line motion can only be observed above a certain threshold voltage. Hence, a slower rising voltage will result in a larger delay in the measured lens response. The time constant of the device further adds to the input voltage rise time-dependent delay.

Simulation Results. The response of the 3.95 mm lens for varying input voltage rise time is simulated using COMSOL Multiphysics 5.2a by solving the Navier–Stokes equation for

DOI: 10.1021/acs.langmuir.7b00631
Langmuir 2017, 33, 4863–4869

two incompressible fluids using a moving mesh boundary. The simulation predicts the time evolution of the fluid velocity and pressure distribution. In addition, the simulations provide insight into the evolution of the liquid−liquid interface profile as a function of time for a given input voltage rise time. The time lapse velocity magnitude of the liquid−liquid interface for a rise time of 10 ms input exponential voltage is shown in Figure 7.

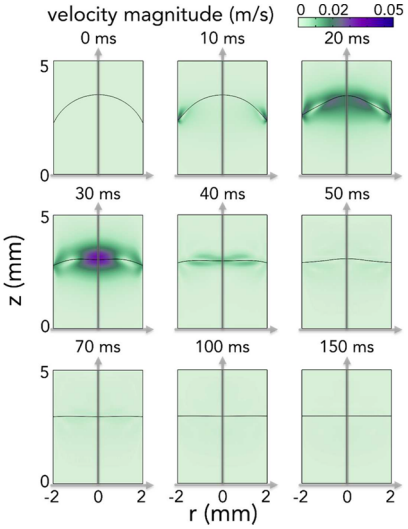

Figure 7. Time lapse of the velocity magnitude for a 3.95 mm diameter lens driven by a 10 ms input exponential voltage from 0 to 28 V. Evolution of the liquid−liquid interface (solid black line) represents the standing wave motion long after the input voltage is reached at 28 V.

A wave is generated at the sidewalls as a result of the contact line motion, and it takes ∼30 ms to reach the center of the lens (see Figure 7). For a 10 ms input rise time voltage, the contact line moves along the sidewall for approximately 70 ms. The contact line motion produces a radially inward wave, which interferes with the reflected wave moving radially outward, resulting in a standing wave that is damped by the viscosity of the liquids. The liquid−liquid interface finally settles to its steady state at approximately 120 ms.

The simulations were compared to the experimental results by simulating the exact experimental conditions. Figure 8a shows the motion of the meniscus on the axis of the lens as a function of time for varying input voltage rise times, and Figure 8b shows the comparison between experimental and simulation results for 3.95 mm lenses using 10 ms input rise time exponential voltage. The simulation result is shifted by 15 ms to match the experimental data. The delay is introduced by the *RC* characteristics of the device and not modeled in COMSOL. The experimental results are in good agreement with the simulation. The simulated and measured photodetector signal oscillations are shown in Figure 8b. Small amplitude variations are due to the uncertainty in the measured distances of the experimental setup.

Effect of the Two-Exponential Input Voltage Drive. Many input shaping techniques have been developed to optimize the response of nonlinear systems. For instance, input shaping techniques in the form of overdriven voltage have been used to reduce the response times of liquid-crystal displays[31] and electrowetting devices.[22,23,25] In our approach, we have studied multiple exponential driving voltages to enhance the response time of the EWOD lenses.

Our method resembles the Posicast control method used in underdamped oscillatory systems.[32,33] To improve the response time of our lenses, we have used a two-exponential driving voltage, as depicted in Figure 9a as a solid line. A 3.95 mm inner diameter lens was actuated from 0 to 31 V, with steady-state contact angles with applied voltage experimentally determined as 155° at 0 V and 90° at 31 V DC. Using a combination of two exponentials as the drive voltage, one must determine the two amplitudes and two rise times in addition to the width of the first exponential voltage, as labeled in Figure 9a. Five unknown variables can be reduced to four using the ratio of the amplitudes of the two exponential driving voltages. To find the optimum driving voltage, we fixed the rise times of the two exponentials to 2 and 5 ms, respectively. Shorter rise times (<15 ms) were chosen to achieve a fast contact line motion upon actuation. The remaining two variables were determined by experimentally actuating the device with various ratios of the amplitudes and widths of the first exponential voltage to find the fastest response time. The response time for single-exponential (dashed line) and two-exponential (solid line) driving voltage is plotted in Figure 9b. We experimentally determined that driving the lens with a single-exponential voltage, τ = 2 ms, from 0 to 31 V results in a response time of 167 ms, whereas actuating the same lens with two exponential voltages (ratio = A_1/A_2 = 8.12; ω_1 = 25 ms; τ_1 = 2 ms; and τ_2 = 5 ms) enhanced the response time to 98 ms. This is a 41% improvement compared to the 2 ms single-exponential drive and a 29% improvement compared to the fastest response obtained for the 3.95 mm inner diameter lens driven using a single-exponential input voltage with a rise time of 15 ms. The significant reduction in the response time can be explained through the destructive interference of two standing waves

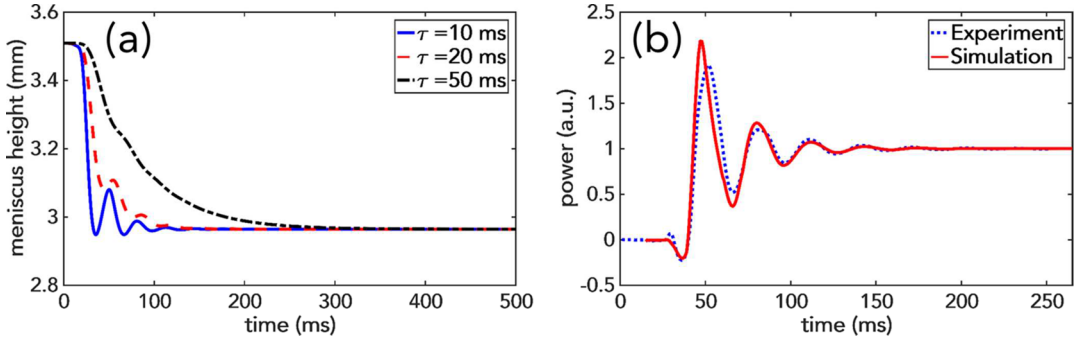

Figure 8. Simulation results for the 3.95 mm diameter lens: (a) motion of the meniscus on the axis of the lens as a function of time for varying input voltage rise times and (b) comparison between the simulation and experimental results for an input voltage rise time of 10 ms.

DOI: 10.1021/acs.langmuir.7b00631
Langmuir 2017, 33, 4863−4869

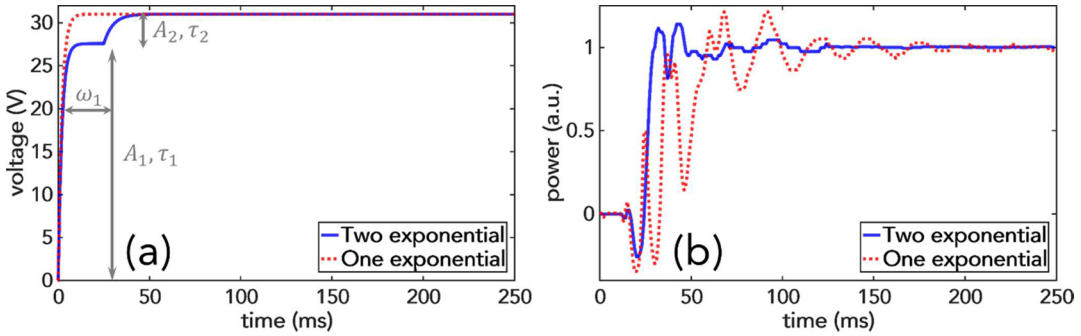

Figure 9. (a) One and two exponential driving voltages are plotted as a function of time with ratio = A_1/A_2 = 27.6/3.4, ω_1 = 25 ms, τ_1 = 2 ms, and τ_2 = 5 ms for the two-exponential driving voltage. The single-exponential driving voltage has a rise time of 2 ms with an amplitude of 31 V. In the two-exponential case, we have fixed the two rise times and varied the ratio of the amplitudes and width, ω_1. (b) Experimental results for single- and two-exponential driving voltage. The solid line shows the fastest response time of 98 ms. Using a 2 ms single-exponential drive voltage results in a response time of 167 ms (dashed line). Using two exponential driving voltages improves the response time by 41% in addition to suppressing the oscillations in the response.

generated by the two exponential rise time functions. The first 2 ms input rise time function generates a rapid contact line motion, which generates a standing wave moving from the sidewall toward the axis of the lens, which upon reflection starts propagating toward the sidewall. The second 5 ms input rise time function generated after a delay generates another standing wave that moves toward the axis of the lens, destructively interferes with the first wave, and dampens the oscillations at the liquid−liquid interface. In addition to this improvement in the response time, the oscillations are suppressed, making the lens behave more like a critically damped system.

Enhancing the response time of electrowetting-based devices using voltage-shaping techniques is important for many applications. We have discussed a few applications in the Introduction, such as optical switches, depth scanning microscopy, and beam steering, that can greatly benefit from faster response time EWOD devices. In addition, employing tools, such as genetic algorithms, can further enhance the optimization process for multiple exponential input voltages and can be used for other arbitrary-shaped input voltages.

CONCLUSION

The dynamics of EWOD lenses using one and two exponential input voltages is investigated, followed by experimental and simulation results. We have studied 2.45 and 3.95 mm diameter lenses filled with 1 wt % SDS in water solution and dodecane. The response times of both lenses were characterized using single-exponential voltage functions with various rise times. The response characteristics of the liquid−liquid interface for the 3.95 mm diameter lens is simulated and compared to the experimental results for single-exponential input voltage. We further improved the response time of a 3.95 mm lens by combining two exponential driving voltages, which shows a response time of 98 ms, indicating a 29% enhancement when compared to the fastest response obtained using single-exponential driving voltage. Our systematic study of carefully controlling the input voltage to drive the EWOD lens provides insight into the importance of the actuation method of EWOD lenses for many applications.

AUTHOR INFORMATION

Corresponding Author

*E-mail: omkar.supekar@colorado.edu.

ORCID

Omkar D. Supekar: 0000-0003-1777-8508

Author Contributions

†Omkar D. Supekar and Mo Zohrabi contributed equally to this work and are listed alphabetically.

Notes

The authors declare no competing financial interest.

ACKNOWLEDGMENTS

The authors are grateful to Robert Cormack and Dr. Joseph Brown for technical discussions. This work was supported by the Office of Naval Research (ONR, W0014-14-1-2739), National Science Foundation (NSF) Instrument Development for Biological Research (IDBR) Grant DBI-1353757, NSF NSC-FO Grant CBET 1631704, and Defense Advanced Research Projects Agency (DARPA)/Microsystems Technology Office (MTO) W31P4Q-14-1-0006, under the CAMS program.

REFERENCES

(1) Mugele, F.; Baret, J.-C. Electrowetting: From Basics to Applications. *J. Phys.: Condens. Matter* **2005**, *17*, R705−R774.

(2) Berge, B.; Peseux, J. Variable focal lens controlled by an external voltage: An application of electrowetting. *Eur. Phys. J. E: Soft Matter Biol. Phys.* **2000**, *3*, 159−163.

(3) Smith, N. R.; Abeysinghe, D. C.; Haus, J. W.; Heikenfeld, J. Agile wide angle beam steering with electrowetting microprisms. *Opt. Express* **2006**, *14*, 6557−6563.

(4) Montoya, R. D.; Underwood, K.; Terrab, S.; Watson, A. M.; Bright, V. M.; Gopinath, J. T. Large extinction ratio optical electrowetting shutter. *Opt. Express* **2016**, *24*, 9660.

(5) Shahini, A.; Xia, J.; Zhou, Z.; Zhao, Y.; Cheng, M. M. C. Versatile Miniature Tunable Liquid Lenses Using Transparent Graphene Electrodes. *Langmuir* **2016**, *32*, 1658−1665.

(6) Shahini, A.; Zeng, P.; Zhao, Y.; Cheng, M. M. C. Individually tunable liquid lens arrays using transparent graphene for compound eye applications. *IEEE MEMS* **2016**, 597−600.

(7) Park, I. S.; Yang, J. W.; Oh, S. H.; Chung, S. K. Multifuctional liquid lens for high-performance miniature cameras. *IEEE MEMS* **2016**, 776−779.

(8) Lee, J.; Park, Y.; Oh, S. H.; Chung, S. K. Multifunctional liquid lens (MLL) for variable focus and variable aperture. *IEEE MEMS* **2017**, 781−784.

(9) Heikenfeld, J.; Smith, N.; Dhindsa, M.; Zhou, K.; Kilaru, M.; Hou, L.; Zhang, J.; Kreit, E.; Raj, B. Recent Progress in Arrayed Electrowetting Optics. *Opt. Photonics News* **2009**, *20*, 20.

(10) Hayes, R. A.; Feenstra, B. J. Video-speed electronic paper based on electrowetting. *Nature* **2003**, *425*, 383−385.

DOI: 10.1021/acs.langmuir.7b00631
Langmuir 2017, 33, 4863−4869

(11) Fair, R. B. Digital microfluidics: Is a true lab-on-a-chip possible? *Microfluid. Nanofluid.* **2007**, *3*, 245−281.
(12) Chang, Y. H.; Lee, G. B.; Huang, F. C.; Chen, Y. Y.; Lin, J. L. Integrated polymerase chain reaction chips utilizing digital microfluidics. *Biomed. Microdevices* **2006**, *8*, 215−225.
(13) Abdelgawad, M.; Freire, S. L. S.; Yang, H.; Wheeler, A. R. All-terrain droplet actuation. *Lab Chip* **2008**, *8*, 672.
(14) Murali, S.; Thompson, K. P.; Rolland, J. P. Three-dimensional adaptive microscopy using embedded liquid lens. *Opt. Lett.* **2009**, *34*, 145−147.
(15) Ozbay, B. N.; Losacco, J. T.; Cormack, R.; Weir, R.; Bright, V. M.; Gopinath, J. T.; Restrepo, D.; Gibson, E. A. Miniaturized fiber-coupled confocal fluorescence microscope with an electrowetting variable focus lens using no moving parts. *Opt. Lett.* **2015**, *40*, 2553−2556.
(16) Jackel, J. L.; Hackwood, S.; Beni, G. Electrowetting optical switch. *Appl. Phys. Lett.* **1982**, *40*, 4−5.
(17) Murade, C. U.; Oh, J. M.; van den Ende, D.; Mugele, F. Electrowetting driven optical switch and tunable aperture. *Opt. Express* **2011**, *19*, 15525−15531.
(18) Day, R.; Lacot, E.; Stoeckel, F.; Berge, B. Three-dimensional sensing based on a dynamically focused laser optical feedback imaging technique. *Appl. Opt.* **2001**, *40*, 1921−1924.
(19) Sundaram, S.; Knapczyk, M.; Temkin, H. All-optical switch based on digital micromirrors. *IEEE Photonics Technol. Lett.* **2003**, *15*, 807−809.
(20) Annapragada, S. R.; Dash, S.; Garimella, S. V.; Murthy, J. Y. Dynamics of droplet motion under electrowetting actuation. *Langmuir* **2011**, *27*, 8198−8204.
(21) Hong, J.; Kim, Y. K.; Kang, K. H.; Oh, J. M.; Kang, I. S. Effects of drop size and viscosity on spreading dynamics in DC electrowetting. *Langmuir* **2013**, *29*, 9118−9125.
(22) Chae, J. B.; Hong, J.; Lee, S. J.; Chung, S. K. Enhancement of response speed of viscous fluids using overdrive voltage. *Sens. Actuators, B* **2015**, *209*, 56−60.
(23) Hong, S. J.; Hong, J.; Seo, H. W.; Lee, S. J.; Chung, S. K. Fast Electrically Driven Capillary Rise Using Overdrive Voltage. *Langmuir* **2015**, *31*, 13718−13724.
(24) Chen, L.; Bonaccurso, E. Electrowetting - From statics to dynamics. *Adv. Colloid Interface Sci.* **2014**, *210*, 2−12.
(25) Berge, B.; Broutin, J.; Gaton, H.; Malet, G.; Simon, E.; Thieblemont, F. Liquid lens based on electrowetting: Actual developments on larger aperture and multiple electrodes design for image stabilization or beam steering. *Proc. SPIE* **2013**, *8616*, 861612.
(26) Kim, Y.; Lee, J. S.; Won, Y. H. Analyzing effects of aperture size and applied voltage on the response time. *Proc. SPIE* **2016**, *9760*, 97600Y.
(27) Kuiper, S.; Hendriks, B. H. W. Variable-focus liquid lens for miniature cameras. *Appl. Phys. Lett.* **2004**, *85*, 1128−1130.
(28) Lippmann, G. Relations entre les phénomènes électriques et capillaires. *Ann. Chim. Phys.* **1875**, *5*, 494.
(29) Raj, B.; Dhindsa, M.; Smith, N. R.; Laughlin, R.; Heikenfeld, J. Ion and Liquid Dependent Dielectric Failure in Electrowetting Systems. *Langmuir* **2009**, *25*, 12387−12392.
(30) Bocquet, L.; Charlaix, E. Nanofluidics, from bulk to interfaces. *Chem. Soc. Rev.* **2010**, *39*, 1073−1095.
(31) Cho, Y.; Park, C.; Bhowmik, A.; Lee, S. New overdrive technology for liquid-crystal displays with a simple architecture. *Opt. Eng.* **2010**, *49* (3), 034001.
(32) Smith, O. J. M. Posicast Control of Damped Oscillatory Systems. *Proc. IRE* **1957**, *45*, 1249−1255.
(33) Robertson, M. J.; Singhose, W. E. Multi-level optimization techniques for designing digital input shapers. *Proc. Am. Control Conf.* **2001**, *1*, 269−274.

DOI: 10.1021/acs.langmuir.7b00631
Langmuir 2017, 33, 4863−4869